



# Constructing Core-Shell Co@N-Rich Carbon Additives Toward Enhanced Hydrogen Storage Performance of Magnesium Hydride

Ke Wang<sup>1</sup> and Qibo Deng<sup>2,3,4\*</sup>

<sup>1</sup> School of Materials Science and Engineering, University of Shanghai for Science and Technology, Shanghai, China,

<sup>2</sup> Institute for New Energy Materials & Low-Carbon Technologies, School of Materials Science and Engineering, Tianjin University of Technology, Tianjin, China, <sup>3</sup> Research Institute for Structure Technology of Advanced Equipment, School of Mechanical Engineering, Hebei University of Technology, Tianjin, China, <sup>4</sup> Key Laboratory of Advanced Energy Materials Chemistry (Ministry of Education), College of Chemistry, Nankai University, Tianjin, China

## OPEN ACCESS

### Edited by:

Hai-Wen Li,  
Kyushu University, Japan

### Reviewed by:

Claudio Pistidda,  
Helmholtz Centre for Materials and  
Coastal Research (HZG), Germany  
Jacques Huot,  
Université du Québec à  
Trois-Rivières, Canada  
Hiroki Miyaoka,  
Hiroshima University, Japan

### \*Correspondence:

Qibo Deng  
qibodeng@tjut.edu.cn

### Specialty section:

This article was submitted to  
Inorganic Chemistry,  
a section of the journal  
Frontiers in Chemistry

Received: 07 January 2020

Accepted: 09 March 2020

Published: 07 April 2020

### Citation:

Wang K and Deng Q (2020)  
Constructing Core-Shell Co@N-Rich  
Carbon Additives Toward Enhanced  
Hydrogen Storage Performance of  
Magnesium Hydride.  
Front. Chem. 8:223.  
doi: 10.3389/fchem.2020.00223

Magnesium hydride (MgH<sub>2</sub>) is regarded as a promising solid-state hydrogen storage material, on account of its moderate price and high gravimetric capacity. However, MgH<sub>2</sub>'s inferior kinetic of hydrogen release impedes its widespread application. In this work, we use core-shell Co@N-rich carbon (CoNC) additive as catalysts to ameliorate the performances of MgH<sub>2</sub>. The surface morphologic structures and hydrogen desorption kinetics of different MgH<sub>2</sub>-CoNC composites are systematically studied. We find that MgH<sub>2</sub>-5 wt% CoNC with carbon contents of 17% (CoNC0) composites exhibit better hydrogen desorption performance. At 325°C, the MgH<sub>2</sub>-5 wt% CoNC0 composites can release up to 6.58 wt% of H<sub>2</sub> in 5 min, which is much higher than 0.3 wt% for pure MgH<sub>2</sub>. Our results demonstrate that importing the core-shell structured catalysts can effectively enhance the hydrogen release kinetics.

**Keywords:** magnesium hydride, hydrogen storage performance, core-shell (C-S) nanostructures, carbon additives, dehydrogenation kinetics

## INTRODUCTION

Low-cost manufacturing, safe storage, and transportation, as well as the effective conversion of hydrogen are the basic requirements for the realization of the large-scale application of hydrogen energy (Baykara, 2018; Abe et al., 2019; Li A. et al., 2019; Staffell et al., 2019; Wei et al., 2019; Xu et al., 2019). Therefore, it is essential to explore a novel and high-capacity hydrogen storage material. Magnesium hydride (MgH<sub>2</sub>) has been considered as a promising hydrogen storage material due to its high hydrogen storage amount of 7.6 wt% and high volumetric hydrogen storage density of 110 kg m<sup>-3</sup> (Aguey-Zinsou and Ares-Fernandez, 2010; Jeon et al., 2011; Shao et al., 2018; Yartys et al., 2019). However, the high hydrogen desorption temperature, sluggish kinetics, and thermodynamics performances of MgH<sub>2</sub> have impeded its further applications.

To enhance the hydrogen adsorption kinetics properties of Mg/MgH<sub>2</sub> materials, three different strategies have been investigated to decrease the dehydrogenation temperature: nano-crystallization (Zhu et al., 2011; Lin et al., 2016; Li et al., 2018), alloying with transition metal (Rusman and Dahari, 2016; Wang et al., 2016; Zhong and Xu, 2019), and catalyst additives (De et al., 2016; Zhang et al., 2018; Liu et al., 2019b; Wang et al., 2019; Wang K. et al., 2019; Zhou et al., 2019a,b). Several papers have demonstrated that using proper catalysts is more convenient

for practical applications (Zhang et al., 2017, 2019; Huang et al., 2018; Valentoni et al., 2018; Chen et al., 2019; Li B. et al., 2019; Hu et al., 2020). Among the catalyst additives, the prominent catalytic influences of Co metal on enhancing the hydrogen desorption properties of  $\text{MgH}_2$  have been reported in previous literature (Mao et al., 2010; Novakovic et al., 2010; Verón et al., 2013; Liu et al., 2018, 2019a). Novakovic et al. have reported that the higher number of d-electrons in Co metal has made it superior to Ti in destabilizing  $\text{MgH}_2$  (Novakovic et al., 2010). Mao et al. proved that the dehydrogenation temperature was lower and the adsorption/desorption kinetics could be enhanced by adding  $\text{CoCl}_2$  catalyst (Mao et al., 2010).  $\text{MgH}_2$ -Co mixture was reported showing better hydrogen storage properties and high-rate hydrogen adsorption/desorption (Verón et al., 2013). Liu et al. have demonstrated that Co@CNTs nano-catalyst doped into  $\text{MgH}_2$  played an essential role in improving its hydrogen storage properties (Liu et al., 2018). A novel bi-metallic Co/Pd@B-CNTs catalyst was also reported recently showing excellent catalytic effects of  $\text{MgH}_2$  at low temperatures (Liu et al., 2019a). Based on literature, the mixture of Co metal and carbon material exhibits effectively catalytic function. It is well-known that the morphology and micro-structure of materials is one of the significant factors to further improve its physical or chemical performance. In comparison with the bulk structure, the core-shell structure exhibits much higher specific surface area for exposed active sites and the more electronic interaction of core and shell material. Different constituent of core and shell can be modulated as a parameter to exhibit the optimal synergistic effect. Herein, we introduced the core-shell Co@N-rich carbon hybrids as catalyst additives into  $\text{MgH}_2$  system to effectively improve the hydrogen desorption performances of  $\text{MgH}_2$ . The carbon shell can protect Co core from oxidation and aggregation. The core-shell structure could further significantly enhance the intimate interface between Co@C and  $\text{MgH}_2$ , providing more active "catalytic sites" and hydrogen "diffusion channels" to reduce the dehydrogenation temperature. Such benefits of additives with core-shell structure then improve the dehydrogenation kinetics of  $\text{MgH}_2$ . Our study also compared the effect of different carbon contents and found that the  $\text{MgH}_2$ -5 wt% CoNC with the carbon contents of 17% (CoNC0) composites had the lowest dehydrogenation temperature and best dehydrogenation kinetic properties.

## MATERIALS AND METHODS

The chemical agents used in this work were purchased from Adamas. Core-shell Co@N-rich carbon hybrids were synthesized according to our previous work (An et al., 2017). The obtained sample with the carbon contents of 17% was designated as CoNC0, and the sample with the carbon amount of 25% was designated as CoNC1. The purchased  $\text{MgH}_2$  was mixed with 3 or 5 wt% of CoNC0 and CoNC1 hybrids through ball-milling at room temperature for 5 h at 450 rpm under 2 MPa  $\text{H}_2$  pressure. The mass ratio of big or small balls and powder was about 40:1.

The surface morphological structures of CoNC and various  $\text{MgH}_2$ -CoNC composites were determined by transmission

electron microscopy (TEM). The thermal decomposition of various  $\text{MgH}_2$ -CoNC composites was studied on differential scanning calorimetry (DSC) and temperature programmed desorption (TPD). The test conditions of DSC measurement were as follows: heating rate of 2, 5, 10, and  $15^\circ\text{C min}^{-1}$ , shielding and sweeping gas of high-purity Ar with  $30\text{ ml min}^{-1}$  flow rate, respectively. As for TPD, the Ar flow rate was  $35.1\text{ ml min}^{-1}$  and the measured temperature was  $50\text{--}500^\circ\text{C}$ . The isothermal hydrogen desorption properties were characterized by a self-made Sieverts-type instrument under an initial pressure of 0.05 MPa hydrogen at 275, 300, and  $325^\circ\text{C}$ , respectively. After complete dehydrogenation, the pressure increased to 0.08 MPa.

## RESULTS AND DISCUSSION

Figure 1 displays the DSC curves of pure  $\text{MgH}_2$  and various  $\text{MgH}_2$ -CoNC composites to investigate the thermal decomposition properties at a heating rate of  $5^\circ\text{C min}^{-1}$ . Obviously, the onset and hydrogen desorption temperatures of  $\text{MgH}_2$ -CoNC composites are lower than that of pure  $\text{MgH}_2$ , demonstrating that the addition of CoNC hybrids can improve the hydrogen desorption kinetics of  $\text{MgH}_2$ . The value of the onset and hydrogen desorption temperatures for these  $\text{MgH}_2$ -CoNC composites are listed in Table 1. The onset temperature

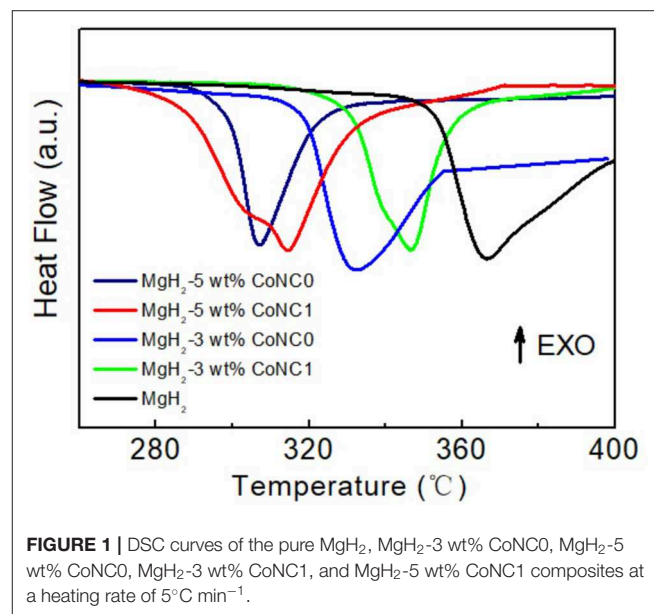


**FIGURE 1** | DSC curves of the pure  $\text{MgH}_2$ ,  $\text{MgH}_2$ -3 wt% CoNC0,  $\text{MgH}_2$ -5 wt% CoNC0,  $\text{MgH}_2$ -3 wt% CoNC1, and  $\text{MgH}_2$ -5 wt% CoNC1 composites at a heating rate of  $5^\circ\text{C min}^{-1}$ .

**TABLE 1** | The onset and peak temperatures of the  $\text{MgH}_2$  and various  $\text{MgH}_2$ -CoNC composites.

Sample	Onset temperature ( $^\circ\text{C}$ )	Peak temperature ( $^\circ\text{C}$ )
$\text{MgH}_2$	344	367
$\text{MgH}_2$ -3 wt% CoNC0	313	332
$\text{MgH}_2$ -5 wt% CoNC0	285	307
$\text{MgH}_2$ -3 wt% CoNC1	312	346
$\text{MgH}_2$ -5 wt% CoNC1	269	314

suggests the dehydrogenation starting. As displayed in **Figure 1**, there is a broad hydrogen desorption peak during the heating process in  $\text{MgH}_2$ ,  $\text{MgH}_2$ -3 wt% CoNC1,  $\text{MgH}_2$ -3 wt% CoNC0, and  $\text{MgH}_2$ -5 wt% CoNC1 composites, suggesting the sluggish hydrogen desorption kinetics. As for the remaining  $\text{MgH}_2$ -5 wt% CoNC0 composites, there is only one sharp peak, located at  $307^\circ\text{C}$ , further implying the enhanced hydrogen desorption kinetics. Moreover, there are two endothermic peaks observed in the case of  $\text{MgH}_2$ -3 wt% CoNC1 and  $\text{MgH}_2$ -5 wt% CoNC1 samples. The identification of two peaks may be due to bimodal particle size distribution formed during ball-milling. This issue can be reduced when increasing the ball-milling time.

In order to further illustrate the impacts of the CoNC additives on the hydrogen desorption properties of  $\text{MgH}_2$ , TPD measurements have been conducted (**Figure 2**). There are two hydrogen desorption peaks of the  $\text{MgH}_2$ -5 wt% CoNC1 composites in the pyrolysis procedure, which can be ascribed to the uneven distribution of the particles after the addition of CoNC1 hybrids (**Figure 2A**). The peak temperatures of  $\text{MgH}_2$ -5 wt% CoNC0,  $\text{MgH}_2$ -5 wt% CoNC1,  $\text{MgH}_2$ -3 wt% CoNC0,

$\text{MgH}_2$ -3 wt% CoNC1, and pure  $\text{MgH}_2$  are 293, 304, 324, 336, and  $348^\circ\text{C}$ , respectively. Obviously, the peak temperatures of the  $\text{MgH}_2$ -CoNC composites are lower than that of pure  $\text{MgH}_2$ . Similarly, the onset temperatures for the above four composites are lower than that of pure  $\text{MgH}_2$ , illustrating the improved dehydrogenation kinetics. This observation from TPD results is consistent with the DSC results. Compared with the pure  $\text{MgH}_2$ , the dehydrogenation amount of the four  $\text{MgH}_2$ -CoNC composites was almost the same (**Figure 2B**), due to the fact that the CoNC hybrids are non-active materials for hydrogen adsorption. Among all the samples, the  $\text{MgH}_2$  with 5 wt% CoNC0 additives exhibits the decreased hydrogen desorption temperature. Therefore, after comprehensive analysis,  $\text{MgH}_2$ -5 wt% CoNC0 composites have been regarded as the optimal material for hydrogen storage in this study.

The surface morphological structures of CoNC0 additives and  $\text{MgH}_2$ -5 wt% CoNC0 composites are characterized and the corresponding TEM images are shown in **Figure 3**. CoNC0 hybrids display a core-shell structure with a Co core (18 nm) coated with N-rich carbon shell. More details on core-shell

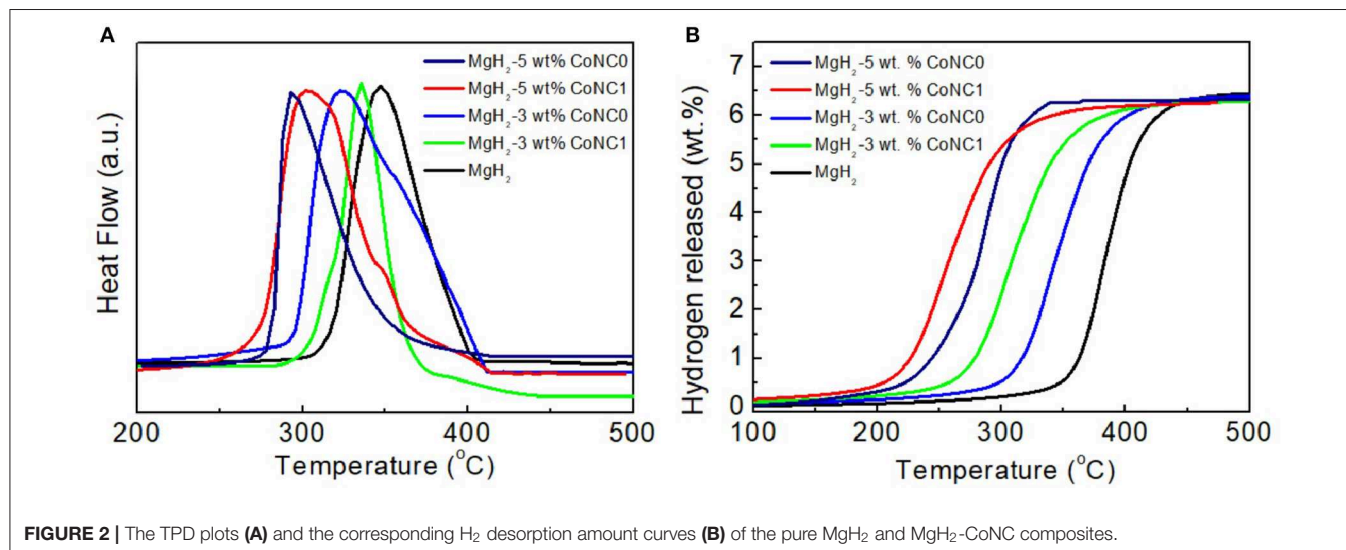


**FIGURE 2** | The TPD plots (A) and the corresponding  $\text{H}_2$  desorption amount curves (B) of the pure  $\text{MgH}_2$  and  $\text{MgH}_2$ -CoNC composites.

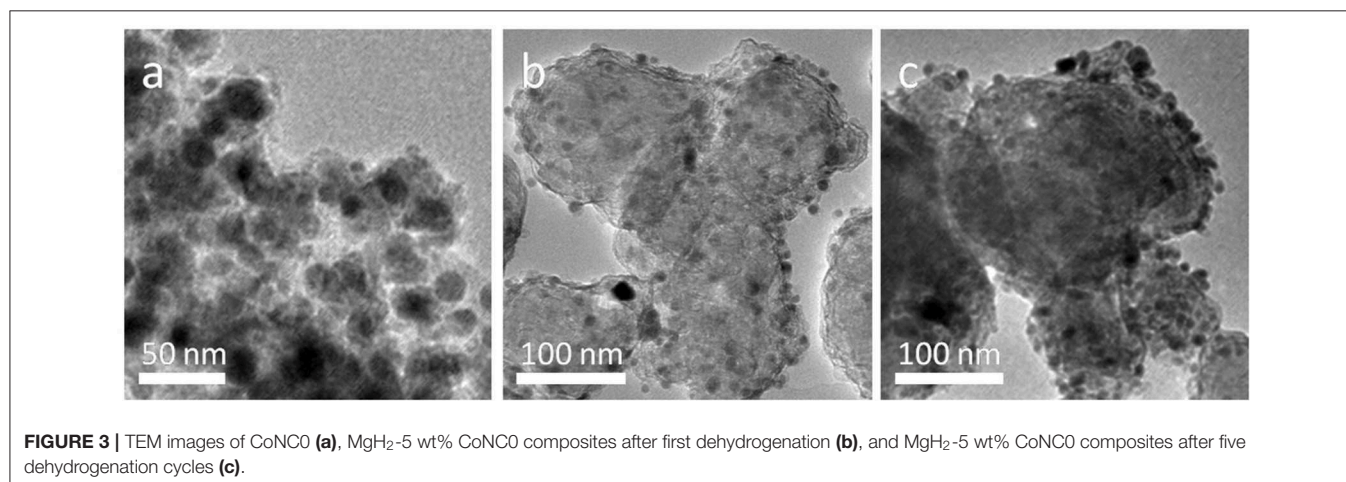


**FIGURE 3** | TEM images of CoNC0 (a),  $\text{MgH}_2$ -5 wt% CoNC0 composites after first dehydrogenation (b), and  $\text{MgH}_2$ -5 wt% CoNC0 composites after five dehydrogenation cycles (c).

structure of hybrids are available in our previous report (An et al., 2017). The TEM images of MgH<sub>2</sub>-5 wt% CoNC0 composites after first dehydrogenation and five cycles are also presented in **Figure 3**. The MgH<sub>2</sub>-5 wt% CoNC0 composites after first dehydrogenation (**Figure 3b**) showed irregular morphologies of accumulated nanoparticles (~30 nm in diameter). Likewise, after five cycles, the anomalous morphology and structure of the MgH<sub>2</sub>-5 wt% CoNC0 composites have been retained while the size of the nanoparticles have increased apparently (**Figure 3c**). The morphological changes after dehydrogenation can be explained by the disaggregation, spreading, nucleation, development, and re-separation procedures of the nanoparticles during hydrogen adsorption-desorption process. The interface migration, disintegration, and incorporation of various phases have been referred to this process, in which the formation of

metal hydride would lead to the rapid increase of nanoparticle size after several hydrogen adsorption-desorption cycles.

To gain a deeper understanding on the enhanced dehydrogenation kinetics of MgH<sub>2</sub>-5 wt% CoNC0 composites, the hydrogen desorption kinetics plots at different temperatures (275, 300, and 325°C) are obtained (**Figure 4**). At the same temperature (300°C), the dehydrogenation amount of MgH<sub>2</sub>-5 wt% CoNC0 composites can reach up to 3.49 wt% in 5 min while the amount is only 0.05 wt% for pure MgH<sub>2</sub>. Even though the reaction time is extended to 50 min, the dehydrogenation amount of pure MgH<sub>2</sub> reaches a value of 1.51 wt%, which is still lower than that of MgH<sub>2</sub>-5 wt% CoNC0 composites in 5 min. The slope for MgH<sub>2</sub>-5 wt% CoNC0 composites is much larger than that of pure MgH<sub>2</sub>, further demonstrating that the addition of CoNC0 hybrids has a prominent influence on the dehydrogenation kinetics of pure MgH<sub>2</sub>. As for MgH<sub>2</sub>-5 wt% CoNC0 composites, the dehydrogenation temperature has a significant impact on the hydrogen desorption amount. Specifically, the hydrogen desorption amount of MgH<sub>2</sub>-5 wt% CoNC0 composites at 325 and 275°C are 6.58 wt% and 0.26 wt% in 5 min, respectively, which increases nearly 25 times.

The above results have further demonstrated that the CoNC0 additives could enhance the dehydrogenation kinetic performances of MgH<sub>2</sub>. Next, the activation energy of hydrogen desorption for MgH<sub>2</sub>-5 wt% CoNC0 composites is investigated by DSC measurements at various heating rate. There is only one endothermic peak of the MgH<sub>2</sub>-5 wt% CoNC0 composites at various heating rate (**Figure 5A**). The temperatures of hydrogen desorption process of MgH<sub>2</sub>-5 wt% CoNC0 composites are 298, 307, 330, and 354°C at a heating rate of 2, 5, 10, and 15°C min<sup>-1</sup>, respectively. The activation energy of MgH<sub>2</sub>-5 wt% CoNC0 composites is then calculated according to the following equation:

$$-\frac{E_a}{R} = \frac{d[\ln(\frac{\beta}{T_p^2})]}{d(\frac{1}{T_p})}$$

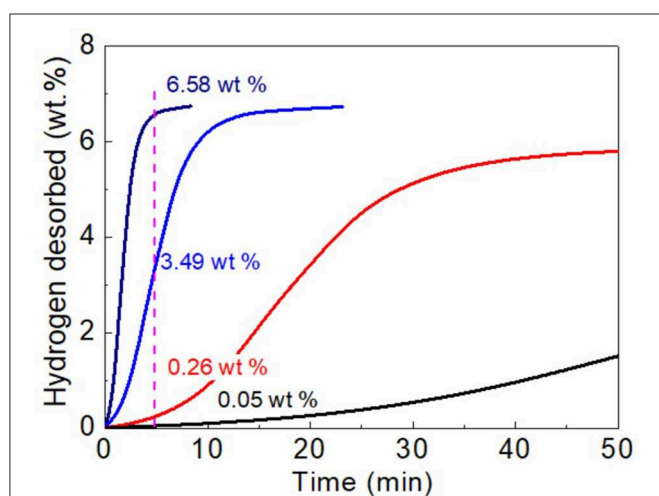


**FIGURE 4** | Hydrogen desorption kinetics curves of pure MgH<sub>2</sub> at 300°C (black line), MgH<sub>2</sub>-5 wt% CoNC0 at 275°C (red line), MgH<sub>2</sub>-5 wt% CoNC0 at 300°C (blue line), and MgH<sub>2</sub>-5 wt% CoNC0 at 325°C (navy line).

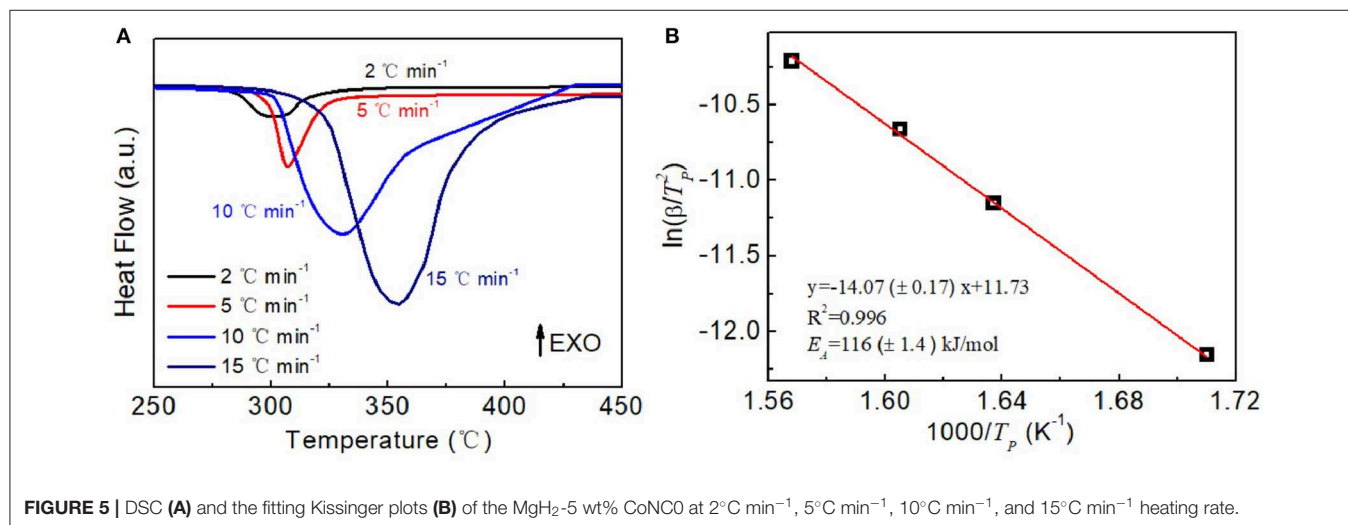


**FIGURE 5** | DSC (A) and the fitting Kissinger plots (B) of the MgH<sub>2</sub>-5 wt% CoNC0 at 2°C min<sup>-1</sup>, 5°C min<sup>-1</sup>, 10°C min<sup>-1</sup>, and 15°C min<sup>-1</sup> heating rate.



According to the fitting result,  $\ln(\beta/T_p^2)$  depends linearly on  $1/T_p$ , which is consistent with the Kissinger plot (Figure 5B). Based on the fitted slope of the Kissinger plot and the constant  $R$ , the activation energy  $E_a$  is determined to be  $116 \pm 1.4 \text{ kJ mol}^{-1}$ . The  $E_a$  value of  $\text{MgH}_2$ -5 wt% CoNC0 composites is comparable to the values for the materials reported previously, such as  $\text{MgH}_2$ -10 wt% CoB/CNTs ( $119 \text{ kJ mol}^{-1}$ ) (Gao et al., 2017), MgNCG ( $137 \text{ kJ mol}^{-1}$ ) (Liu et al., 2016),  $\text{MgH}_2$ -TiN ( $144 \text{ kJ mol}^{-1}$ ) (Wang et al., 2015), and  $\text{MgH}_2$ - $\text{FeCl}_3$  ( $130 \text{ kJ mol}^{-1}$ ) (Ismail et al., 2014). These results further manifest the prominent effects of the Co@C additives on enhancing the dehydrogenation kinetics of pure  $\text{MgH}_2$ . However, the  $E_a$  value of  $\text{MgH}_2$ -5 wt% CoNC0 is higher than  $53.4 \text{ kJ mol}^{-1}$  of FeCo nanosheets,  $67.64 \text{ kJ mol}^{-1}$  of  $\text{TiO}_2$  nanosheets,  $82.2 \text{ kJ mol}^{-1}$  of  $\text{ZrMn}_2$  nanoparticle, and  $99 \text{ kJ mol}^{-1}$  of  $\text{VNbO}_5$  in the current literature (Valentoni et al., 2018; Yang et al., 2019; Zhang et al., 2019; Zhang M. et al., 2019). Lower activation energies could be due to the intrinsic catalytic activities of different additives with high surface energy. Comparing with many reported dopants, the simple preparation of CoNC composite and relatively inexpensive raw materials in our study may be advantageous to decrease the cost of product for practical application. The properties reported in this work could naturally be enhanced via optimizing the constituent structure, for example, the amount of the Co and the diameter of the core-shell nanoparticles, which will be the future research direction. It is also interesting to fabricate the core-shell structured catalyst additives with high catalytic activity in a simple preparation procedure for the hydrogen energy storage in a future study.

## CONCLUSION

To summarize,  $\text{MgH}_2$ - $x$  wt% Co@NC (Co@NC0 and Co@NC1) ( $x = 3, 5$ ) composites were synthesized via ball-milling method. The microstructure, dehydrogenation kinetics of the  $\text{MgH}_2$ - $x$  wt% Co@NC composites and the influences of Co@NC additives on the hydrogen desorption kinetics of  $\text{MgH}_2$  materials are discussed. Based on the experimental results, the addition

of Co@NC additives has promoted the hydrogen desorption kinetics of  $\text{MgH}_2$ . In addition, the  $\text{MgH}_2$ -5 wt% CoNC0 composite exhibits the lowest hydrogenation temperature and maintains a moderate dehydrogenation amount. The  $\text{MgH}_2$ -5 wt% Co@NC0 composites generate 6.58 wt% hydrogen in 5 min at  $325^\circ\text{C}$  and 3.49 wt% hydrogen in 5 min at  $300^\circ\text{C}$ . Moreover, according to the Kissinger plot, the calculated  $E_a$  of the  $\text{MgH}_2$ -5 wt% Co@NC0 composites is about  $116 \text{ kJ mol}^{-1}$ , indicating that the Co@NC hybrids have effectively promoted the hydrogen adsorption kinetics of  $\text{MgH}_2$ . Our work imports the core-shell microstructure to play a positive role on the hydrogen storage performance of magnesium hydride and then provides useful guidance for the future development of advanced materials for hydrogen storage.

## DATA AVAILABILITY STATEMENT

All datasets generated for this study are included in the article/supplementary material.

## AUTHOR CONTRIBUTIONS

KW performed the experiments, analyzed the data, and wrote the original draft. QD designed the experiments and reviewed manuscript. KW and QD revised manuscript. All authors discussed the results and commented on the manuscript.

## ACKNOWLEDGMENTS

All authors thank Prof. Cuihua An for the helpful discussions and the assistance on experiments. KW thanks the support from the Program of Shanghai Pujiang Program (No. 18PJ1409100), the Natural Science Foundation of University of Shanghai for Science and Technology (No. ZR18PY05), and the program for Professor of Special Appointment (Eastern Scholar) at Shanghai Institutions of Higher Learning. QD thanks the support from the Hundred Talents Program of Tianjin University of Technology.

## REFERENCES

- Abe, J. O., Popoola, A. P. I., Ajenifuja, E., and Popoola, O. M. (2019). Hydrogen energy, economy and storage: review and recommendation. *Int. J. Hydrogen Energy* 44, 15072–15086. doi: 10.1016/j.ijhydene.2019.04.068
- Aguey-Zinsou, K. F., and Ares-Fernandez, J. R. (2010). Hydrogen in magnesium: new perspectives toward functional stores. *Energy Environ. Sci.* 3, 526–543. doi: 10.1039/b921645f
- An, C. H., Wang, M. Y., Li, W. Q., Deng, Q. B., Wang, Y. J., Jiao, L. F., et al. (2017). Mesoporous Co@N-rich carbon hybrids for a high rate aqueous alkaline battery. *Electrochim. Acta* 250, 135–142. doi: 10.1016/j.electacta.2017.08.060
- Baykara, S. Z. (2018). Hydrogen: a brief overview on its sources, production and environmental impact. *Int. J. Hydrogen Energy* 43, 10605–10614. doi: 10.1016/j.ijhydene.2018.02.022
- Chen, M., Hu, M. M., Xie, X. B., and Liu, T. (2019). High loading nanoconfinement of V-decorated Mg with 1 nm carbon shells: hydrogen storage properties and catalytic mechanism. *Nanoscale* 11, 10045–10055. doi: 10.1039/C8NR09909J
- De, S., Zhang, J. G., Luque, R., and Yan, N. (2016). Ni-based bimetallic heterogeneous catalysts for energy and environmental applications. *Energy Environ. Sci.* 9, 3314–3347. doi: 10.1039/C6EE02002J
- Gao, S. C., Liu, H. Z., Xu, L., Li, S. Q., Wang, X. H., and Yan, M. (2017). Hydrogen storage properties of nano-CoB/CNTs catalyzed  $\text{MgH}_2$ . *J. Alloys Compd.* 735, 635–642. doi: 10.1016/j.jallcom.2017.11.047
- Hu, M. H., Xie, X. B., Chen, M., Zhu, C. X., and Liu, T. (2020). TiCX-decorated Mg nanoparticles confined in carbon shell: preparation and catalytic mechanism for hydrogen storage. *J. Alloys Compd.* 817:152813. doi: 10.1016/j.jallcom.2019.152813
- Huang, X., Xiao, X. Z., Wang, X. C., Wang, C. T., Fan, X. L., Tang, Z. C., et al. (2018). Synergistic catalytic activity of porous rod-like  $\text{TMTiO}_3$  (TM = Ni and Co) for reversible hydrogen storage of magnesium hydride. *J. Phys. Chem. C* 122, 27973–27982. doi: 10.1021/acs.jpcc.8b10387
- Ismail, M., Juahir, N., and Mustafa, N. S. (2014). Improved hydrogen storage properties of  $\text{MgH}_2$  Co-doped with  $\text{FeCl}_3$  and carbon nanotubes. *J. Phys. Chem. C* 118, 18878–18883. doi: 10.1021/jp5046436
- Jeon, K. J., Moon, H. R., Ruminski, A. M., Jiang, B., Kisielowski, C., Bardhan, R., et al. (2011). Air-stable magnesium nanocomposites provide rapid and high-capacity hydrogen storage without using heavy-metal catalysts. *Nat. Mater.* 10, 286–290. doi: 10.1038/nmat2978

- Li, A., Zhu, W. J., Li, C. C., Wang, T., and Gong, J. L. (2019). Rational design of yolk-shell nanostructures for photocatalysis. *Chem. Soc. Rev.* 48, 1874–1907. doi: 10.1039/C8CS00711J
- Li, B., Li, J. D., Zhao, H. J., Yu, X. Q., and Shao, H. Y. (2019). Mg-based metastable nano alloys for hydrogen storage. *Int. J. Hydrogen Energy* 44, 6007–6018. doi: 10.1016/j.ijhydene.2019.01.127
- Li, J. D., Li, B., Shao, H. Y., Li, W., and Lin, H. J. (2018). Catalysis and downsizing in Mg-based hydrogen storage materials. *Catalysts* 8:89. doi: 10.3390/catal8020089
- Lin, H. J., Zhang, C., Wang, H., Ouyang, L. Z., Zhu, Y. F., Li, L. Q., et al. (2016). Controlling nanocrystallization and hydrogen storage property of Mg-based amorphous alloy via a gas-solid reaction. *J. Alloys Compd.* 658, 272–277. doi: 10.1016/j.jallcom.2016.05.286
- Liu, G., Wang, K. F., Li, J. P., Wang, Y. J., and Yuan, H. T. (2016). Enhancement of hydrogen desorption in magnesium hydride catalyzed by graphene nanosheets supported Ni-CeO<sub>x</sub> hybrid nanocatalyst. *Int. J. Hydrogen Energy* 41, 10786–10794. doi: 10.1016/j.ijhydene.2016.03.205
- Liu, M. J., Xiao, X. Z., Zhao, S. C., Chen, M., Mao, J. F., Luo, B. S., et al. (2019a). Facile synthesis of Co/Pd supported by few-walled carbon nanotubes as an efficient bidirectional catalyst for improving the low temperature hydrogen storage properties of magnesium hydride. *J. Mater. Chem. A* 7, 5277–5287. doi: 10.1039/C8TA12431K
- Liu, M. J., Xiao, X. Z., Zhao, S. C., Saremi-Yarahmadi, S., Chen, M., Zheng, J. G., et al. (2018). ZIF-67 derived Co@CNTs nanoparticles: remarkably improved hydrogen storage properties of MgH<sub>2</sub> and synergetic catalysis mechanism. *Int. J. Hydrogen Energy* 44, 1059–1069. doi: 10.1016/j.ijhydene.2018.11.078
- Liu, M. J., Zhao, S. C., Xiao, X. Z., Chen, M., Sun, C. H., Yao, Z. D., et al. (2019b). Novel 1D carbon nanotubes uniformly wrapped nanoscale MgH<sub>2</sub> for efficient hydrogen storage cycling performances with extreme high gravimetric and volumetric capacities. *Nano Energy* 61, 540–549. doi: 10.1016/j.nanoen.2019.04.094
- Mao, J., Guo, Z., Yu, X., Liu, H., Wu, Z., and Ni, J. (2010). Enhanced hydrogen sorption properties of Ni and Co-catalyzed MgH<sub>2</sub>. *Int. J. Hydrogen Energy* 35, 4569–4575. doi: 10.1016/j.ijhydene.2010.02.107
- Novakovic, N., Novakovic, J. G., Matovic, L., Manasjjevic, M., Radisavljevic, I., Mamula, B. P., et al. (2010). Ab initio calculations of MgH<sub>2</sub>, MgH<sub>2</sub>:Ti and MgH<sub>2</sub>:Co compounds. *Int. J. Hydrogen Energy* 35, 598–608. doi: 10.1016/j.ijhydene.2009.11.003
- Rusman, N. A. A., and Dahari, M. (2016). A review on the current progress of metal hydrides material for solid-state hydrogen storage. *Int. J. Hydrogen Energy* 41, 12108–12126. doi: 10.1016/j.ijhydene.2016.05.244
- Shao, H. Y., He, L. Q., Lin, H. J., and Li, H. W. (2018). Progress and trends in magnesium-based materials for energy-storage research: a review. *Energy Technol.* 6, 445–458. doi: 10.1002/ente.201700401
- Staffell, I., Scamman, D., Abad, A. V., Balcombe, P., Dodds, P. E., Ekins, P., et al. (2019). The role of hydrogen and fuel cells in the global energy system. *Energy Environ. Sci.* 12, 463–491. doi: 10.1039/C8EE01157E
- Valentoni, A., Mulas, G., Enzo, S., and Garroni, S. (2018). Remarkable hydrogen storage properties of MgH<sub>2</sub> doped with VNbO<sub>5</sub>. *Phys. Chem. Chem. Phys.* 20, 4100–4108. doi: 10.1039/C7CP07157D
- Verón, M. G., Condó A. M., and Gennari, F. C. (2013). Effective synthesis of Mg<sub>2</sub>CoH<sub>5</sub> by reactive mechanical milling and its hydrogen sorption behavior after cycling. *Int. J. Hydrogen Energy* 38, 973–981. doi: 10.1016/j.ijhydene.2012.10.086
- Wang, H., Lin, H. J., Cai, W. T., Ouyang, L. Z., and Zhu, M. (2016). Tuning kinetics and the thermodynamics of hydrogen storage in light metal element based systems- a review of recent process. *J. Alloys Compd.* 658, 280–300. doi: 10.1016/j.jallcom.2015.10.090
- Wang, K., Zhang, X., Ren, Z. H., Zhang, X. L., Hu, J. J., Gao, M. X., et al. (2019). Nitrogen-stimulated superior catalytic activity of niobium oxide for fast full hydrogenation of magnesium at ambient temperature. *Energy Storage Mater.* 23, 79–87. doi: 10.1016/j.ensm.2019.05.029
- Wang, Y., Zhang, Q. Y., Wang, Y. J., Jiao, L. F., and Yuan, H. T. (2015). Catalytic effects of different Ti-based materials on dehydrogenation performances of MgH<sub>2</sub>. *J. Alloys Compd.* 645, S509–S512. doi: 10.1016/j.jallcom.2014.12.071
- Wang, Z. Y., Zhang, X. L., Ren, Z. H., Liu, Y., Hu, J. J., Li, H. W., et al. (2019). In situ formed ultrafine NbTi nanocrystals from a NbTiC solid-solution MXene for hydrogen storage in MgH<sub>2</sub>. *J. Mater. Chem. A* 7, 14244–14252. doi: 10.1039/C9TA03665B
- Wei, C., Rao, R. R., Peng, J. Y., Huang, B. T., Stephens, I. E. L., Risch, M., et al. (2019). Recommended practices and benchmark activity for hydrogen and oxygen electrocatalysis in water splitting and fuel cells. *Adv. Mater.* 31:1806296. doi: 10.1002/adma.201806296
- Xu, H. M., Ci, S. Q., Ding, Y. C., Wang, G. X., and Wen, Z. H. (2019). Recent advances in precious metal-free bifunctional catalysts for electrochemical conversion systems. *J. Mater. Chem. A* 7, 8006–8029. doi: 10.1039/C9TA00833K
- Yang, X. L., Ji, L., Yan, N. H., Sun, Z., Lu, X., Zhang, L. T., et al. (2019). Superior catalytic effects of FeCo nanosheets on MgH<sub>2</sub> for hydrogen storage. *Dalton Trans.* 48, 12699–12706. doi: 10.1039/C9DT02084E
- Yartys, V. A., Lototsky, M. V., Akiba, E., Albert, R., Antonov, V. E., Ares, J. R., et al. (2019). Magnesium based materials for hydrogen based energy storage: past, present and future. *Int. J. Hydrogen Energy* 44, 7809–7859. doi: 10.1016/j.ijhydene.2018.12.212
- Zhang, J. G., Shi, R., Zhu, Y. F., Liu, Y. N., Zhang, Y., Li, S. S., et al. (2018). Remarkable synergistic catalysis of Ni-doped ultrafine TiO<sub>2</sub> on hydrogen sorption kinetics of MgH<sub>2</sub>. *ACS Appl. Mater. Interfaces* 10, 24975–24980. doi: 10.1021/acsami.8b06865
- Zhang, L. T., Cai, Z. L., Yao, Z. D., Ji, L., Sun, Z., Yan, N. H., et al. (2019). A striking catalytic effect of facile synthesized ZrMn<sub>2</sub> nanoparticles on the de/rehydrogenation properties of MgH<sub>2</sub>. *J. Mater. Chem. A* 7, 5626–5634. doi: 10.1039/C9TA00120D
- Zhang, L. T., Chen, L. X., Fan, X. L., Xiao, X. Z., Zheng, J. G., and Huang, X. (2017). Enhanced hydrogen storage properties of MgH<sub>2</sub> with numerous hydrogen diffusion channels provided by Na<sub>2</sub>Ti<sub>3</sub>O<sub>7</sub> nanotubes. *J. Mater. Chem. A* 5, 6178–6185. doi: 10.1039/C7TA00566K
- Zhang, M., Xiao, X. Z., Wang, X. W., Chen, M., Lu, Y. H., Liu, M. J., et al. (2019). Excellent catalysis of TiO<sub>2</sub> nanosheets with high-surface-energy {001} facets on the hydrogen storage properties of MgH<sub>2</sub>. *Nanoscale* 11, 7465–7473. doi: 10.1039/C8NR10275A
- Zhong, H. C., and Xu, J. B. (2019). Tuning the de/hydrating thermodynamics and kinetics of Mg by mechanical alloying with Sn and Zn. *Int. J. Hydrogen Energy* 44, 2926–2933. doi: 10.1016/j.ijhydene.2018.11.173
- Zhou, C. S., Bowman, R. C., Fang, Z. Z., Lu, J., Xu, L., Sun, P., et al. (2019a). Amorphous TiCu-based additives for improving hydrogen storage properties of magnesium hydride. *ACS Appl. Mater. Interfaces* 11, 38868–38879. doi: 10.1021/acsami.9b16076
- Zhou, C. S., Fang, Z. G. Z., Sun, P., Xu, L., and Liu, Y. (2019b). Capturing low-pressure hydrogen using V-Ti-Cr catalyzed magnesium hydride. *J. Power Sources* 413, 139–147. doi: 10.1016/j.jpowsour.2018.12.048
- Zhu, C., Hosokai, S., and Akiyama, T. (2011). Growth mechanism for the controlled synthesis of MgH<sub>2</sub>/Mg crystals via a vapor-solid process. *Cryst. Growth Des.* 11, 4166–4174. doi: 10.1021/cg200733b

**Conflict of Interest:** The authors declare that the research was conducted in the absence of any commercial or financial relationships that could be construed as a potential conflict of interest.

Copyright © 2020 Wang and Deng. This is an open-access article distributed under the terms of the Creative Commons Attribution License (CC BY). The use, distribution or reproduction in other forums is permitted, provided the original author(s) and the copyright owner(s) are credited and that the original publication in this journal is cited, in accordance with accepted academic practice. No use, distribution or reproduction is permitted which does not comply with these terms.